British Journal of Pharmacology

British Journal of Pharmacology (2017) **174** 1797–1809 1797

RESEARCH PAPER

Mathematical modelling of the drug release from an ensemble of coated pellets

Correspondence Gaetano Lamberti, Department of Industrial Engineering, University of Salerno, Fisciano, SA 84084, Italy.
E-mail: glamberti@unisa.it

Received 15 November 2016; **Revised** 27 February 2017; **Accepted** 27 February 2017

Diego Caccavo[1], Gaetano Lamberti[1], Maria Margherita Cafaro[1], Anna Angela Barba[2], Jurgita Kazlauske[3] and Anette Larsson[4,5]

[1]Department of Industrial Engineering, University of Salerno, Fisciano, SA, Italy, [2]Department of Pharmacy, University of Salerno, Fisciano, SA, Italy, [3]AstraZeneca R&S, Mölndal, Sweden, [4]Pharmaceutical Technology, Department of Chemical Engineering, Chalmers University of Technology, Gothenburg, Sweden, and [5]SuMo BIOMATERIALS, A VINNOVA VINN Excellence Center, Chalmers University of Technology, Gothenburg, Sweden

BACKGROUND AND PURPOSE

Coated pellets are widely used as oral drug delivery systems, being highly accepted by patients and with several advantages compared to single unit devices. However, their behaviour needs to be elucidated so as to improve the effectiveness of the formulations and reduce production costs. In spite of this important issue, few mathematical modelling studies have been attempted, mostly due to the complexities arising from the system's polydispersity (non-homogeneous multiple-unit particulate systems), which has been scarcely investigated using mechanistic models.

EXPERIMENTAL APPROACH

A mechanistic mathematical model was developed that was able to describe the single pellet behaviour in terms of hydration, drug dissolution, diffusion and release and particle size. This model was then extended to describe and predict the behaviour of mono- and polydispersed ensembles of pellets.

KEY RESULTS

The polydispersity arising from the size and distribution of the inert core was shown to have a minimal effect on the drug release profile, whereas the thickness and distribution of the polymeric film was found to be the key parameter determining the drug release.

CONCLUSIONS AND IMPLICATIONS

The mechanistic model developed, which is capable of determining the polydispersity of the drug delivery system, was able to predict the release kinetics from ensembles of pellets and to highlight the key parameters that need to be controlled in the production of pellet-based drug delivery systems, demonstrating its use as a powerful predictive tool.

Abbreviations

HPMC, hydroxypropyl methylcellulose; ICs, initial conditions; ODEs, ordinary differential equations; PSD, particle size distribution; SD, size distribution

DOI:10.1111/bph.13776

Introduction

Generalities

The oral route for drug administration is one of the most commonly used methods to deliver drugs due to high patient compliance and the large mass-exchange surface available in the gastrointestinal tract. Many oral pharmaceuticals are prepared as multiple-unit particulate systems, as these offer several advantages over a single unit device. These multi-unit systems reduce the local drug concentration and are less likely to result in gastric irritation (Grassi *et al.,* 2006), have faster gastric emptying and longer residence time in the intestine (Abrahamsson *et al.,* 1996). Among the particulate systems, coated pellets are most often used to obtain controlled drug release. The insoluble polymer layer covers the pellets, finely modulates the drug release, masks any undesirable taste of the drug and improves its stability by protecting the inner part from the external environment (Siepmann *et al.,* 2008).

State of the art

The modelling of ensembles of coated pellets is a complicated task due to the polydispersed character of non-homogeneous multiple-unit particulate systems, and few mathematical modelling studies have been attempted. Dappert and Thies (1978) with their statistical-based model, followed by Gross *et al.* (1986) and Donbrow *et al.* (1988), have demonstrated that the cumulative release of a polydispersed system does not characterize the basic release mechanism, and they clearly showed that the form of the release profile from a single pellet differs from the release profile of an ensemble. Dappert and Thies (1978) also demonstrated that the cumulative amount of drug released from a particular ensemble of polydispersed particles can be deduced from the cumulative release of each particle class. A particle class defines a dimensional range in which a certain number or mass (numerical or mass distribution) of particles can be individuated. The particles in each class can be described by the average dimension of the class (i.e. mean diameter). In their model, the mutual interaction between particle classes was disregarded. Grassi *et al.* (2000) utilized a mechanistic model to analyse the drug release from an ensemble of swellable, cross-linked polymer particles with a known initial particle size distribution (PSD). Borgquist *et al.* (2002; 2004) developed a mechanistic model to describe drug release from ensembles of coated pellets but ignored the interaction between the dimensional classes of pellets. Other models have been attempted and some of these are reported in Kaunisto *et al.* (2011). However, most of these mechanistic studies have ignored the interaction between ensembles of particles with the same size, namely, 'classes', that is, they assumed the drug released from one class does not influence the drug release from the other classes (perfect sink condition), and considered the polydispersity generated only by difference in internal drug core radius, disregarding variations in the thickness of the polymer film. To our knowledge, a mathematical model able to describe the mass fraction evolution of all the species along with the system deformation, accounting for the size distribution (SD) of the different layers has never been proposed in the case of coated pellets.

Aims

There are two aims in this present study. The first is to develop a mechanistic (or first principles) mathematical model able to describe the drug dissolution and release, as well as the system deformation, from a single pellet made of an inert core, a drug and a polymer layer. The second is to describe the behaviour of an ensemble of mono- and polydispersed pellets through the extension of the single pellet model. The polydispersity will be considered as potentially arising from the SD of each pellet layer.

Methods

The materials and methods used to produce the coated pellets and test the drug release will be briefly reported.

Materials

The inert cores of pellets were made of microcrystalline cellulose spheres (Cellets® 500, Syntapharm GmbH, Germany). Anhydrous theophylline, our model drug, was bought from Sigma-Aldrich (St. Louis, MO, USA). Hydroxypropyl methylcellulose (HPMC) 5 cP, used as plasticizer within the drug layer, was a gift from Dow Chemical (Midland, MI, USA). The coating was made of Surelease®E-7-19 020, aqueous ethyl cellulose dispersion (24.7% ww^{-1}, Colorcon, Harleysville, PA, USA). Sodium phosphate monobasic monohydrate and disodium phosphate for the preparation of buffered release medium were bought from Sigma-Aldrich (St. Louis, MO, USA).

Production of coated pellets

The pellets analysed in this work were produced by the solution/suspension layering technique, which requires a starter core (nucleation seed) to promote the process. The coating was performed in a fluid bed coater equipped with a Wurster column (Gandalf 0, AstraZeneca, Sweden) in two steps. In the first step, the Cellets spheres (starter core) were coated with a theophylline : HPMC solution (90:10 ww^{-1}) to produce the drug layer. In the second step, the drug-covered pellets were coated with the aqueous ethyl cellulose dispersion to obtain the polymeric film layer. The theophylline : HPMC (weight ratio 90:10) solution was sprayed onto microcrystalline cores. These coated pellets were sprayed with ethyl cellulose layers using Surelease (15% ww^{-1}) at an inlet temperature of 45°C and cured at 50°C for 24 h in an oven. The operative conditions were chosen to produce a theoretical drug layer thickness of 12 μm and theoretical polymeric film thickness of 20, 30 and 60 μm respectively (f_t20, f_t30, f_t60). The theoretical film thickness in microns is denoted as f_tx, where x is the thickness value.

Drug release

Drug release from an ensemble of pellets, 500 mg, was analysed in a USP II apparatus (Varian 705DS, Varian Inc., Palo Alto, CA, USA) at 37°C, 100 rpm in 1 L of phosphate buffer (pH 6.8). Samples of 3 mL were automatically collected (8000 Dissolution sampling station, Agilent Technologies, Santa Clara, CA, USA) and analysed by a spectrophotometer

(Cary 60 UV-Vis, Agilent Technologies, Santa Clara, CA, USA) at 272 nm to calculate the drug concentration in the medium and the drug release profiles.

Surelease film properties

Diffusivity measurements. The diffusivity of the water and theophylline within the polymeric film was measured in a diffusion cell with a donor and an acceptor compartment separated by a square piece (1.5 × 1.5 cm) of the polymeric film. The amount of tritium-labelled water and theophylline passing from the donor to the acceptor compartment were monitored, respectively, with a scintillation counter (TriCarb 2810TR, PerkinElmer, Walthalm, MA, USA) and a spectrophotometer (Cary 60 UV-Vis, Agilent Technologies, Santa Clara, CA, USA) at 272 nm.

Swelling of Surelease free film. Three free films of Surelease with a weight of 36.1 ± 4.2 mg and a thickness of 141.8 ± 9.6 μm were put in 100 mL of distilled water at 37°C and hydrated. The films were withdrawn at different times, in the interval 0–80 h, and weighed to determine the weight variation attributed to the amount of water absorbed.

Particle size distribution of Cellets

The PSD of Cellets 500 was estimated with a laser scattering granulometer (Mastersizer 3000, Malvern, Worcestershire, UK), equipped with the Hydro EV apparatus to create wet dispersions. Distilled water was used as the dispersant.

Polymer and drug thickness layers

The thickness of the polymeric layer was measured by analysing cross sections of the pellets. The procedure to obtain pellets cross sections for the SEM images is the following: The pellets were immobilized in paraffin wax and cut with a cryostat-microtome (Electronic cryostat Cryotome E, Thermo Electron Corporation, Runcorn, UK). Cross sections of the pellets were analysed with an optical microscope (Leica DMLP, Leica Microsystems, Milan, Italy); these were obtained by immobilizing the pellets in polyester resin (Solver Italia, Salerno, Italy) and cutting with a semi-automated rotary microtome (Leica RM2245, Leica Microsystems, Milan, Italy).

Modelling

Phenomenology. A pellet is depicted schematically in Figure 1. The phenomenological hypotheses are the following:

- The water from the external environment (Ω_D) diffuses into the pellet through the coating (Ω_C), which swells ($R_C(t)$ increases), causing hydration of the internal parts;
- The drug and the HPMC dissolve, with the same kinetics, from the solid layer (Ω_A: $R_A(t)$ decreases) into the liquid layer (Ω_B: $R_B(t)$ increases);
- The dissolved drug from the liquid layer diffuses through the polymeric coating (Ω_C) and accumulates in the external environment (Ω_D);
- Meanwhile, the liquid layer continues to increase in volume due to the water coming in from Ω_C ($R_B(t)$ increases), causing the stretching of the polymeric coating Ω_C ($R_C(t) - R_B(t)$ decreases) due to its limited capacity to swell.

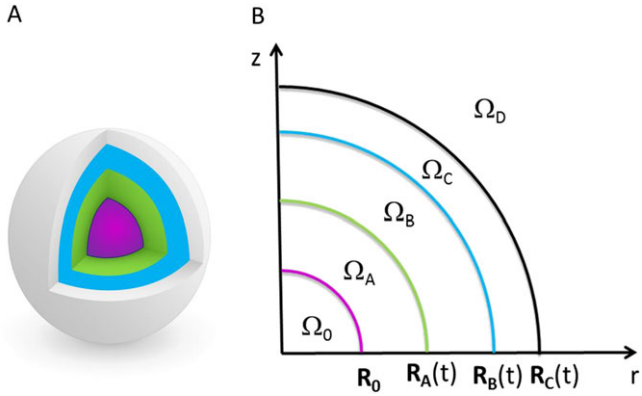

Figure 1

3D representation of a pellet (A) with its 2D axisymmetric schematization (B). Ω_0 represents the inert core (Cellets) with fixed radius R_0. Ω_A represents the solid drug layer (drug and HPMC) with the time-dependent outer radius $R_A(t)$. Ω_B represents the dissolved drug layer (drug, HPMC and water) with time-dependent outer radius $R_B(t)$. Ω_C represents the polymeric film layer (Surelease, drug and water) with the time-dependent outer radius $R_C(t)$. Ω_D represents the dissolution medium (drug and water) in which the pellet is immersed.

Although it has been observed, experimentally, that the Cellets swell in PBS resulting in an increased radius by about 10% in this model, this phenomenon is disregarded, because the water reaches the core only once the drug layer has been completely dissolved and almost completely released. The inclusion of this effect, even if it is not difficult to be implement, would require other parameters to be defined – like the water diffusivity and the MCC/water equilibrium constant – that are not easily available and would add little in terms of depiction of real behaviour. Osmotic pressure driven release, which is manifested in the case of polymeric film as pores/cracks, is not considered in this work.

Single pellet modelling. The system is described with a lumped approach, so that each domain has a homogeneous value of mass fraction of each species. In each domain, the mass balances for the *N*-1 species, where *N* is the total number of species, as well as the total mass balance are written and solved for the species mass fractions and the domain dimensions respectively. In the following, the species are indicated with the subscripts 1 (water), 2 (theophylline), 3 (HPMC) and 4 (Surelease). The domain at which the variable is referring to is indicated with a superscript letter. The model parameters, discussed in the following, are presented in Table 1.

Domain Ω_A. The domain Ω_A represents the solid theophylline/HPMC layer. In this domain, the mass fraction of drug and polymer are constant and equal to the initial value: $\omega_2^A = \omega_{20}^A = 0.9$ and $\omega_3^A = \omega_{30}^A = 0.1$. Since the mass fractions are fixed, the domain density (ρ^A) is constant, and the mass balance on a species is sufficient to describe the

system deformation ($R_A(t)$). The mass balance on the dissolving drug can be written using the Noyes and Whitney (1897) equation:

$$\frac{dm_2^A}{dt} = \frac{d\left(\rho^A \omega_{20}^A \Omega_A\right)}{dt} = -4\pi R_A^2 k_{diss} \rho^B \left(\omega_{2,sat}^B - \omega_2^B\right) \quad (1)$$
$$R_A(t=0) = R_{A0}$$

$$\frac{1}{\rho^A} = \left(\frac{\omega_{20}^A}{\rho_{20}} + \frac{\omega_{30}^A}{\rho_{30}}\right) = \text{constant} \quad (2)$$

where k_{diss} is the dissolution rate constant, which describes the mass transfer rate from the solid layer into the liquid layer. Following Marucci *et al.* (2013), the dissolution rate can be estimated from the Sherwood correlation for a sphere by $Sh = 2 + 0.6Re^{1/2}Sc^{1/3}$ (Bird *et al.*, 2007) considering that the product $Re^{1/2}Sc^{1/3}$ is very small due to the internal stagnant conditions (Manca and Rovaglio, 2003). Therefore, $Sh = 2$, and thus, $k_{diss} = D_2^B/R_A$. The parameter D_2^B is the theophylline diffusivity in the domain Ω_B, which is a water rich solution with a low percentage of HPMC and theophylline, a situation analogous to the fully swollen matrix of Caccavo *et al.* (2015), from which the value of the D_2^B was taken [1.5×10^{-10} ($m^2 \cdot s^{-1}$)]. The mass fraction $\omega_{2,sat}^B = 0.0115$ represents the theophylline saturation mass fraction at the solid–liquid interface (calculated from the solubility

Table 1

Model parameters

Independent parameters	Value	Description
D_1^B	2.2×10^{-9} ($m^2 \cdot s^{-1}$) (Caccavo *et al.*, 2015)	Water diffusivity in the dissolved drug layer (Ω_B)
D_2^B	1.5×10^{-10} ($m^2 \cdot s^{-1}$) (Caccavo *et al.*, 2015)	Drug diffusivity in the dissolved drug layer (Ω_B)
D_1^C	1.99×10^{-12} ($m^2 \cdot s^{-1}$) (from experiment)	Water diffusivity in the polymeric film (Ω_C)
D_2^C	3.1×10^{-13} ($m^2 \cdot s^{-1}$) (from experiment)	Drug diffusivity in the polymeric film (Ω_C)
D_1^D	3×10^{-9} ($m^2 \cdot s^{-1}$) (Holz *et al.*, 2000)	Water diffusivity in the dissolution medium (Ω_D)
D_2^D	8.21×10^{-10} ($m^2 \cdot s^{-1}$) (Grassi *et al.*, 2001)	Drug diffusivity in the dissolution medium (Ω_D)
$\omega_{2,sat}^B$	0.0115 (−) (Serajuddin and Jarowski, 1985)	Theophylline saturation mass fraction in water
m_1^{BC}	4.95 (−) (from experiment)	Water equilibrium constant: relates the water mass fraction in Ω_C to its equilibrium counterpart in Ω_B
m_1^{CD}	0.2 (−) (from experiment)	Water equilibrium constant: relates the water mass fraction in $\Omega_D$to its equilibrium counterpart in Ω_C
ρ_{10}	1000 ($kg \cdot m^{-3}$) (Caccavo *et al.*, 2015)	Pure water density
ρ_{20}	1200 ($kg \cdot m^{-3}$) (Caccavo *et al.*, 2015)	Pure theophylline density
ρ_{30}	1200 ($kg \cdot m^{-3}$) (Caccavo *et al.*, 2015)	Pure HPMC density
ρ_{40}	1200 ($kg \cdot m^{-3}$)	Pure Surelease density
Dependent parameters	**Expression**	**Description**
k_{diss}	D_2^B/R_A	Theophylline dissolution rate constant
K_1^{BC}	$\left(1/k_1^B + m_1^{BC}/k_1^C\right)^{-1}$	Overall water mass transport coefficient between Ω_B and Ω_C
K_2^{BC}	$\left(1/k_2^B + 1/k_2^C\right)^{-1}$	Overall Theophylline mass transport coefficient between Ω_B and Ω_C
k_1^B	$D_1^B/(R_B - R_A)$	Water mass transport coefficient between Ω_B
k_2^B	$D_2^B/(R_B - R_A)$	Theophylline mass transport coefficient between Ω_B
K_1^{CD}	$\left(1/k_1^C + m_1^{CD}/k_1^D\right)^{-1}$	Overall water mass transport coefficient between Ω_C and Ω_D
K_2^{CD}	$\left(1/k_2^C + 1/k_2^D\right)^{-1}$	Overall Theophylline mass transport coefficient between Ω_C and Ω_D
k_1^C	$D_1^C/(R_C - R_B)$	Water mass transport coefficient between Ω_C
k_2^C	$D_2^C/(R_C - R_B)$	Theophylline mass transport coefficient between Ω_C
k_1^D	D_1^D/R_C	Water mass transport coefficient between Ω_D
k_2^D	D_2^D/R_C	Theophylline mass transport coefficient between Ω_D

in water at 37°C: 11.6 $g.L^{-1}$ (Serajuddin and Jarowski, 1985)).

Domain Ω_B. The domain Ω_B represents the internal liquid layer made of a water solution of HPMC and theophylline. In this layer, the drug enters from Ω_A (due to the solid layer dissolution) and leaves diffusing toward Ω_C (first and second term at right hand side of eq. (3)). The HPMC, eq. (4), can only enter into this domain following the dissolution of the theophylline, but cannot be released (the diffusivity of the HPMC in the Surelease layer goes to zero). Water can enter into this region from the polymer coating, eq. (6), and the total mass of the system and its density vary according to eqs (5) and (7) respectively.

Ω_B and Ω_C, defined in Table 1, which is a time-dependent function related to the parameters D_1^B (from Caccavo *et al.* (2015)), D_1^C (from the experimental results) and to the equilibrium constant m_1^{BC}. The equilibrium constant m_1^{BC} relates the water mass fraction in Ω_C to its equilibrium counterpart in Ω_B: $\omega_{1,eq}^B = m_1^{BC}\omega_{1,eq}^C$. Knowing that $\omega_{1,eq}^C \approx 0.2$ from the Surelease free film swelling tests and considering that $\omega_{1,eq}^B \to 1\ (\tilde{}0.99)$, results in that $m_1^{BC} \to 5$ (being $\omega_{1,eq}^B = m_1^{BC}\omega_{1,eq}^C$ and then $m_1^{BC} = \omega_{1,eq}^B/\omega_{1,eq}^C \tilde{}4.95$). This will allow the entry of water in the domain Ω_B until its mass fraction reaches 99%, which is the equilibrium value. The domain Ω_B at time zero, physically nonexistent, is

$$\frac{dm_2^B}{dt} = \frac{d\left(\rho^B\omega_2^B\Omega_B\right)}{dt} = 4\pi R_A^2 k_{diss}\rho^B\left(\omega_{2,sat}^B - \omega_2^B\right) - 4\pi R_B^2 K_2^{BC}\left(\rho^B\omega_2^B - \rho^C\omega_2^C\right) = \dot{m}_2^B$$
$$\omega_2^B(t=0) = \omega_{20}^B \tag{3}$$

$$\frac{dm_3^B}{dt} = -\frac{dm_3^A}{dt} = \frac{d\left(\rho^B\omega_3^B\Omega_B\right)}{dt} = 4\pi R_A^2\frac{\omega_{30}^A}{\omega_{20}^A}k_{diss}\rho^B\left(\omega_{2,sat}^B - \omega_2^B\right) = \dot{m}_3^B$$
$$\omega_3^B(t=0) = \omega_{30}^B \tag{4}$$

$$\frac{dm^B}{dt} = \frac{d\left(\rho^B\Omega_B\right)}{dt} = \dot{m}_1^B + \dot{m}_2^B + \dot{m}_3^B$$
$$R_B(t=0) = R_{B0} \tag{5}$$

$$\dot{m}_1^B = 4\pi R_B^2 K_1^{BC}\left(m_1^{BC}\,\rho^c\omega_1^c - \rho^B\omega_1^B\right) \tag{6}$$

$$\frac{1}{\rho^B} = \left(\frac{1-\omega_2^B-\omega_3^B}{\rho_{10}} + \frac{\omega_2^B}{\rho_{20}} + \frac{\omega_3^B}{\rho_{30}}\right) \tag{7}$$

The transport parameter K_2^{BC} is the overall time-dependent theophylline mass transport coefficient between Ω_B and Ω_C,

mathematically represented by a very thin layer [3×10^{-9} (μm)] made of pure water, for numerical reasons, to avoid singularities.

Domain Ω_C. This domain represents the polymer coating through which theophylline and water can diffuse. In particular, the theophylline diffuses from the inner layer, the liquid layer Ω_B, and leaves the domain diffusing toward Ω_D (first and second term at right hand side of eq. 8). The Surelease in this case does not enter or leave the system; therefore, its mass is constant, eq. 9, but its mass fraction is not constant. Water can enter or leave this domain from both the dissolution medium (Ω_D) and the liquid layer (Ω_B), eq. 11. The total mass of the system and its density vary according to eqs 10 and 12 respectively.

$$\frac{dm_2^C}{dt} = \frac{d\left(\rho^C\omega_2^C\Omega_C\right)}{dt} = 4\pi R_B^2 K_2^{BC}\left(\rho^B\omega_2^B - \rho^C\omega_2^C\right) - 4\pi R_C^2 K_2^{CD}\left(\rho^C\omega_2^C - \rho^D\omega_2^D\right) = \dot{m}_2^C$$
$$\omega_2^C(t=0) = \omega_{20}^C \tag{8}$$

defined in Table 1, which is a function of the theophylline diffusivities in both the domains: D_2^B (from Caccavo *et al.* (2015)) and D_2^C (from the experimental results). Similarly, K_1^{BC} is the overall water mass transport coefficient between

$$\frac{dm_4^C}{dt} = \frac{d\left(\rho^C\omega_4^C\Omega_C\right)}{dt} = 0 = \dot{m}_4^C$$
$$\omega_4^C(t=0) = \omega_{40}^C \tag{9}$$

$$\frac{dm^C}{dt} = \frac{d(\rho^C \Omega_C)}{dt} = \dot{m}_1^C + \dot{m}_2^C + \dot{m}_4^C \qquad R_C(t=0) = R_{C0} \tag{10}$$

$$\dot{m}_1^C = 4\pi R_C^2 K_1^{CD}\left(m_1^{CD}\,\rho^D\omega_1^D - \rho^C\omega_1^C\right) - 4\pi R_B^2 K_1^{BC}\left(m_1^{BC}\rho^C\omega_1^C - \rho^B\omega_1^B\right) \tag{11}$$

$$\frac{1}{\rho^C} = \left(\frac{1-\omega_2^C-\omega_4^C}{\rho_{10}} + \frac{\omega_2^C}{\rho_{20}} + \frac{\omega_4^c}{\rho_{40}}\right) \tag{12}$$

Likewise K_2^{BC}, the transport parameter K_2^{CD} is the overall theophylline mass transport coefficient between Ω_C and Ω_D, defined in Table 1, which is a time-dependent function related to the parameters D_2^C and D_2^D, this last being the diffusion coefficient of the theophylline in water at 37°C [8.21×10^{-10} ($m^2{\cdot}s^{-1}$) (Grassi *et al.*, 2001)]. K_1^{CD} is the overall water mass transport coefficient between Ω_C and Ω_D, defined in Table 1, which is a time-dependent function related to the parameters D_1^C, D_1^D and m_1^{CD}. D_1^D is the self-diffusion coefficient of water in water at 37°C [3×10^{-9} ($m^2{\cdot}s^{-1}$) (Holz *et al.*, 2000)]. The equilibrium constant m_1^{CD} relates the water mass fraction in Ω_D to its equilibrium counterpart in Ω_C: $\omega_{1,eq}^C = m_1^{CD}\omega_{1,eq}^D$. Knowing, from the Surelease free film swelling tests, that $\omega_{1,eq}^C \approx 0.2$ and considering that $\omega_{1,eq}^D \approx 1$ results in $m_1^{CD} = 0.2$.

Domain Ω_D. The domain Ω_D represents the dissolution medium. Theophylline can reach this domain by diffusing through the polymer coating, eq. 13. The total mass of this domain, eq. 14, can vary due to the exit of water, described by eq. 15, and drug entering.

$$\frac{dm_2^D}{dt} = \frac{d(\rho^D\omega_2^D\Omega_D)}{dt} = 4\pi R_C^2 K_2^{CD}\left(\rho^C\omega_2^C - \rho^D\omega_2^D\right) = \dot{m}_2^D \qquad \omega_2^D(t=0) = \omega_{20}^D \tag{13}$$

$$\frac{dm^D}{dt} = \frac{d(\rho^D\Omega_D)}{dt} = \dot{m}_2^D - \dot{m}_1^D \qquad \Omega_D(t=0) = \Omega_{D0} \tag{14}$$

$$\dot{m}_1^D = 4\pi R_C^2 K_1^{CD}\left(m_1^{CD}\,\rho^D\omega_1^D - \rho^C\omega_1^C\right) \tag{15}$$

$$\frac{1}{\rho^D} = \left(\frac{1-\omega_2^D}{\rho_{10}} + \frac{\omega_2^D}{\rho_{20}}\right) \tag{16}$$

Despite the mass variation of the dissolution medium being negligible in normal dissolution tests where $\Omega_D \gg (\Omega_A+\Omega_B+\Omega_C)$, this might not be negligible in single pellet release tests.

Ensemble of pellets modelling

Homogeneous system. When modelling the drug release from an ensemble of pellets, the first conceivable approach is to consider the whole dose made of perfectly equal pellets (monodispersed system). This assumption requires a minimum variation of the equations presented in the Single pellet modelling section; in particular, the mass balances in the domain Ω_D, eqs 13 and 14, become:

$$\frac{dm_2^D}{dt} = \frac{d(\rho^D\omega_2^D\Omega_D)}{dt} = N_P 4\pi R_C^2 K_2^{CD}\left(\rho^C\omega_2^C - \rho^D\omega_2^D\right) = \dot{m}_2^D \qquad \omega_2^D(t=0) = \omega_{20}^D \tag{17}$$

$$\frac{dm^D}{dt} = \frac{d(\rho^D\Omega_D)}{dt} = \dot{m}_2^D - \dot{m}_1^D\,N_P \qquad \Omega_D(t=0) = \Omega_{D0} \tag{18}$$

where N_P represents the number of pellets in the system.

Heterogeneous system: relevance of the PSD of Cellets. The PSD of Cellets was implemented by considering the radius of the Cellets as a vector ($\mathbf{R_0}$) whose components were the average dimensions of each class. The drug layer thickness ($\mathbf{R_{A0}} \approx \mathbf{R_{B0}}$) was obtained by assuming a homogeneous drug distribution within all the particle classes, generating the same drug layer thickness (calculated in 6.3 μm). The external radii were calculated by assuming that all the sprayed Surelease homogeneously covered the pellets.

$$\mathbf{R_0} = [242,\ 275,\ 313,\ 356,\ 404,\ 459]\mu m \tag{19}$$

$$\mathbf{R_{A0}} = \mathbf{R_0} + 6.3\ \mu m \tag{20}$$

$$\mathbf{R_{C0}} = \mathbf{R_{A0}} + [20 \text{ or } 30 \text{ or } 60]\ \mu m \tag{21}$$

$$\frac{n_i}{n_{tot}} = [0.079,\ 0.335,\ 0.410,\ 0.155,\ 0.020,\ 0.001] \tag{22}$$

The ratio n_i/n_{tot} represents the numerical fraction distribution of the Cellets that also becomes, with the assumptions made, the numerical fraction distribution of the pellets.

In this case, the ODEs given by eqs 1, 3, 4, 5, 8, 9 and 10 have to be solved for each of the six classes, whereas the mass balance in the dissolution medium (Ω_D), eqs 13, 14 and 15, become:

$$\frac{dm_2^D}{dt} = \frac{d(\rho^D\omega_2^D\Omega_D)}{dt} = \sum_i N_i 4\pi R_{C,i}^2 K_{2,i}^{CD}\left(\rho_i^C\omega_{2,i}^C - \rho^D\omega_2^D\right) = \dot{m}_2^D \qquad \omega_2^D(t=0) = \omega_{20}^D \tag{23}$$

$$\frac{dm^D}{dt} = \frac{d(\rho^D\Omega_D)}{dt} = \dot{m}_2^D - \dot{m}_1^D \qquad \Omega_D(t=0) = \Omega_{D0} \tag{24}$$

$$\dot{m}_1^D = \sum_i N_i 4\pi R_{C,i}^2 K_{1,i}^{CD}\left(m_1^{CD}\,\rho^D\omega_1^D - \rho_i^C\omega_{1,i}^C\right) \tag{25}$$

where N_i is the number of pellets in the ith class. Therefore, the system to solve is made of $6\times7+2=44$ ODEs.

Heterogeneous system: relevance of the SD of the coating thickness. Unlike the drug layer thickness, where the average thickness dimension can be estimated from the effective drug loading and the SD is too small to play a crucial rule, the SD of the polymeric coating thickness can have a great influence on drug release. This layer indeed is the limiting step, and it finely moderates the drug transport preventing a burst release. Its thickness, along with its resistance to the species transport, is strongly related to the drug mass flux. Thicker coatings reduce the mass fraction gradient and, hence, the drug mass flux. In contrast, thinner coatings increase the mass fraction gradient and thus the drug mass flux. There is a thickness distribution along a single pellet as well as between pellets, that could be observed from microscopic images.

In the present study, it has been supposed that this intra- and inter-particles film thickness (f_t) distribution can be described using a Gaussian distribution, eq. 26, in which μ and σ represent the mean and the standard deviation of the distribution (the approach is not constrained to this type of distribution; other distribution functions could be implemented to describe the real case). The cumulative distribution function is known, eq. 27, and dividing the interval (0–3 μ) in 10 classes with the same amplitude, it is possible to obtain the numerical fraction of particles in the ith class, eq. 28, of interval $[f_t^*(i+1), f_t^*(i)]$ characterized by the film thickness $f_t^{mean}(i)$, eq. 29. At this point, similarly to the previous case, the radii can be expressed by vectors (of 10 components) where the ith class will be different only for the film thickness, eqs 30–32.

$$q_0(f_t \mid \mu, \sigma) = \frac{1}{\sigma\sqrt{2\pi}} e^{-\frac{(f_t-\mu)^2}{2\sigma^2}} \tag{26}$$

$$Q_0(f_t^* \mid \mu, \sigma) = \int_{-\infty}^{f_t^*} q_0(f_t \mid \mu, \sigma) df_t = \frac{1}{2}\left[1 + \operatorname{erf}\left(\frac{f_t^* - \mu}{\sigma\sqrt{2}}\right)\right] \tag{27}$$

$$\left.\frac{n_i}{n_{tot}}\right|_{f_t^{mean}(i)} = \left[Q_0(f_t^*(i+1) \mid \mu, \sigma) - Q_0(f_t^*(i) \mid \mu, \sigma)\right]\Big|_{i=1\ldots N-1} \tag{28}$$

$$f_t^{mean}(i) = \left.\left(\frac{f_t^*(i+1) + f_t^*(i)}{2}\right)\right|_{i=1\ldots N-1} \tag{29}$$

$$(\mathbf{R_0})_{i=1\ldots 10} = 300\ \mu m \tag{30}$$

$$\mathbf{R_{A0}} = \mathbf{R_0} + 6.3\ \mu m \tag{31}$$

$$\mathbf{R_{C0}} = \mathbf{R_{A0}} + \mathbf{f_t^{mean}}\ \mu m \tag{32}$$

The model thus formulated is a system of 72 ordinary differential equations (ODEs).

Model numerical solution. The model consists of a system of ordinary differential equations (ODEs) that was numerically solved in MATLAB R2014B, with the ode15s solver (Shampine and Reichelt, 1997). The initial conditions for the single pellet model are reported in Table 2, whereas the modification of these conditions for the ensemble of pellets model can be found within the text (Ensemble of pellets modelling section). The MATLAB code is available as Supporting Information.

Results

Experimental results

Drug release from ensembles of pellets. The experimental results showing the drug release of the ensembles of pellets are presented in Figure 2.

The release curves (Figure 2) show a constant release rate (zero-order release) for up to 80% of the drug released, followed by a substantial decrease in the release rate. An increase in the polymeric film thickness decreased the drug release rate.

Surelease film properties

Diffusivity of water and theophylline in the Surelease film. The water and theophylline diffusion coefficients in the Surelease film were of $1.99 \times 10^{-12} \pm 0.14 \times 10^{-12}$ and $3.1 \times 10^{-13} \pm 0.32 \times 10^{-13}$ ($m^2 \cdot s^{-1}$) respectively. These values were used in the model to describe the diffusion of water and drug in the Surelease coating layer (Ω_C), indicated with D_1^C and D_2^C in Table 1.

Swelling of the Surelease film. The recorded increase in the weight in the Surelease free film immersed in distilled water was around 20% $w \cdot w^{-1}$ at equilibrium conditions.

PSD of Cellets. The cumulative mass distribution is presented in Figure 3, calculated by starting from the mass

Table 2

Single pellet model variables with the respective ODE eq. number and the initial value of the variable

Variable	ODE	Initial value
R_A	1	$306–3 \times 10^{-9}$ (μm)
R_B	5	306 (μm)
R_C	10	326* or 336* or 366* (μm)
ω_2^B	3	0
ω_3^B	4	0
ω_2^C	8	0
ω_4^C	9	1
ω_2^D	13	0
Ω_D	14	1 (L)

The radii with the asterisks are theoretical values. It is assumed that all the Surelease sprayed goes onto the pellets

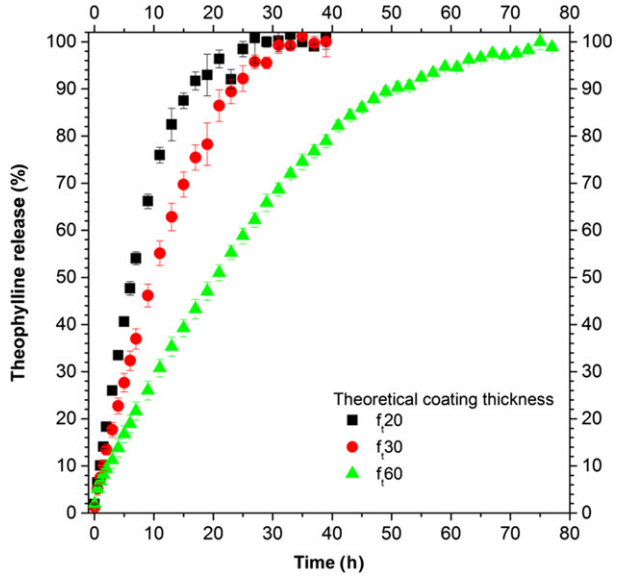

Figure 2
Experimental drug release from ensembles of pellets (500 mg) for three different theoretical coating thicknesses.

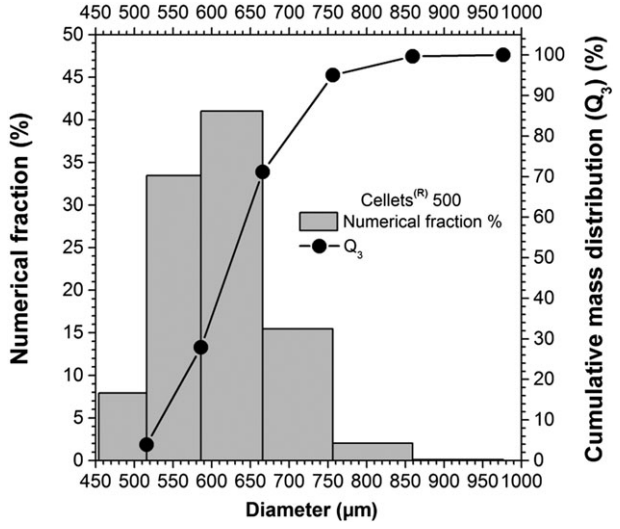

Figure 3
Particle size distribution (PSD) of Cellets 500 in terms of cumulative mass distribution and numerical fraction.

distribution. The results, in accordance with the Cellets producer, show a quite narrow PSD, with the majority of the particles having diameters between 500 and 750 μm. The numerical fraction was used to evaluate the effect of the PSD of the Cellets on the drug release behaviour.

Polymer and drug layer thickness. Both the methods of preparation and analysis, described in the Polymer and drug thickness layers section, to evaluate the thickness of the polymeric layer were able to display an intra- and inter-particle (i.e. between different particles and within the layer covering the same particle) inhomogeneity. This implies the presence of a thickness distribution along a single pellet and between pellets. (Figure 4)

The drug layer thickness was estimated by considering the effective drug mass loaded onto the pellets, which was calculated from the release tests. It was assumed that the ratio of theophylline : HPMC (90:10 $w \cdot w^{-1}$) was constant, when the thickness was calculated for Cellets of the same dimensions (single pellet case, Single pellet modelling section) or for PSDs of Cellets (Ensemble of pellets modelling section). In the latter case, in which the PSDs of Cellets was considered, it was assumed that the thickness of the drug layer was uniform within the PSD classes.

Single pellet model results

The systems of nine ODEs with the initial conditions (ICs) reported in Table 2 were simultaneously solved. The IC for the drug layer radius (R_{A0}) was calculated from the effective drug mass loaded on the pellets, obtained from the drug release tests. IC for the coating layers R_{C0} was calculated by assuming a uniform covering efficiency of 100%. In the following, the radii and the drug mass fraction evolution, which are our main interest, within the system will be shown. However, with this modelling approach, the time evolution of all the other mass fractions as well as the single species mass evolution can be obtained.

The single pellet radii evolutions for a polymer coating thickness of 20 μm (f_t20) are shown in Figure 5. The radius of the solid layer R_A linearly decreases with time until complete dissolution, at the critical time t_c. The liquid layer radius R_B increases mainly due to the water entering. The external pellet radius R_C promptly absorbs water and swells; after that, its size increases due to the increase in the internal liquid layer. This leads to the stretching of the polymeric coating, with a reduction in its thickness ($R_C - R_B$ decreases).

The drug mass fraction evolutions in the domains Ω_B, Ω_C and Ω_D during the dissolution process are presented in Figure 6.

Within the first hour, the drug mass fraction in the liquid layer (ω_2^B) reaches saturation conditions and stays at that value, thanks to the solid layer dissolution, until the critical time t_c. At that point, the solid drug reservoir is finished and the mass fraction starts to decrease. The drug mass fraction in the polymeric coating (ω_2^C) follows the same trend of ω_2^B, reaching a constant value that is a function of the ease of drug transport within the system. The drug mass fraction in Ω_D increases until reaching a constant value that represents the total initial amount of drug in one pellet in 1 L of dissolution medium.

Ensemble of pellets model results

Homogeneous system. This model, constituted by eqs 1–12 and 16–18, was first adjusted to reproduce the experimental results of the pellets with theoretical polymer thickness of 20 μm (f_t20). The drug diffusion in Ω_C was used as the only fitting parameter, and it was increased by a factor 2 to optimize the description of the experimental results. This

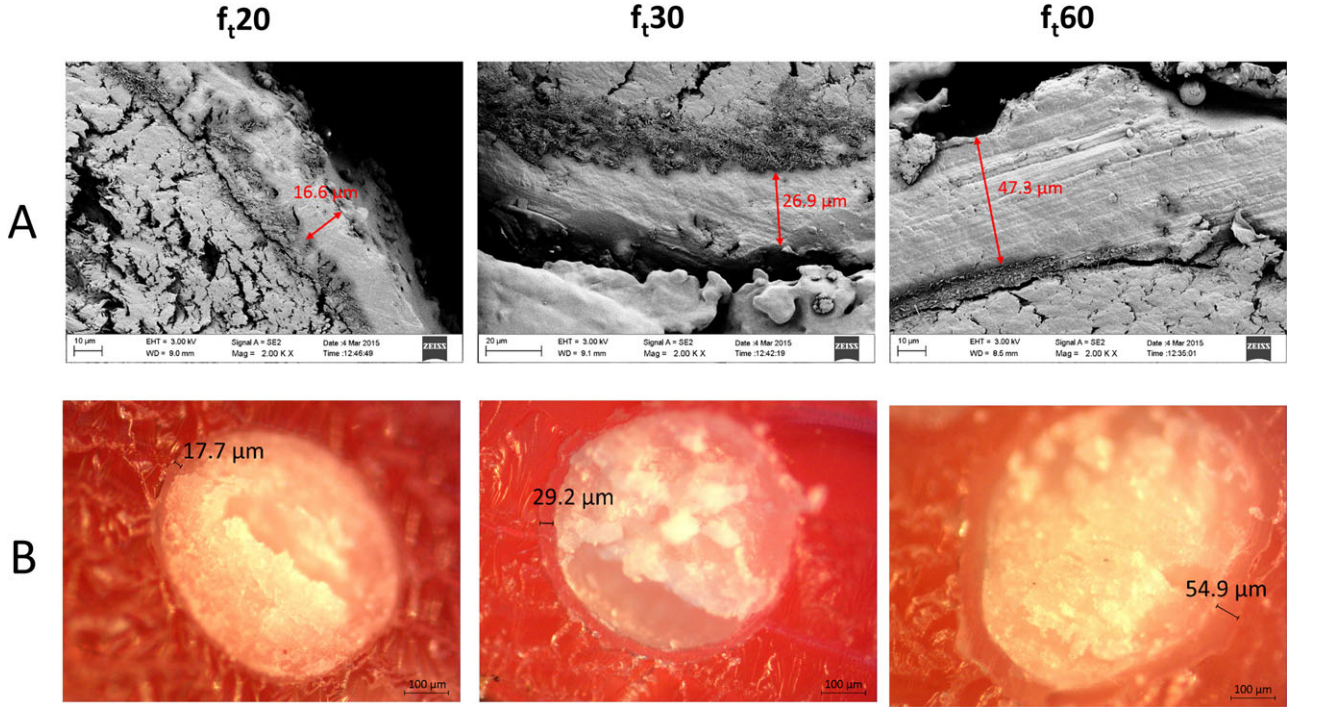

Figure 4

Polymeric layer thickness inhomogeneity. (A) Scanning electron microscope images of pellets cross sections. (B) Optical microscope images of pellet cross sections. Images on the left, centre and right depict pellets with a theoretical film thickness of 20, 30 and 60 µm respectively.

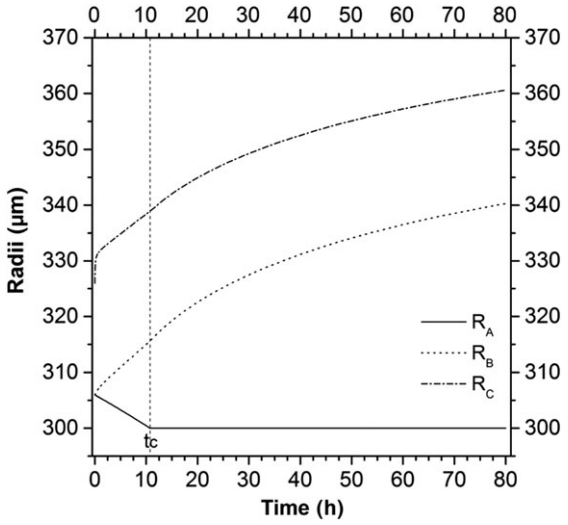

Figure 5

The development of an increased radii during the dissolution process for an initial polymer coating thickness of 20 µm.

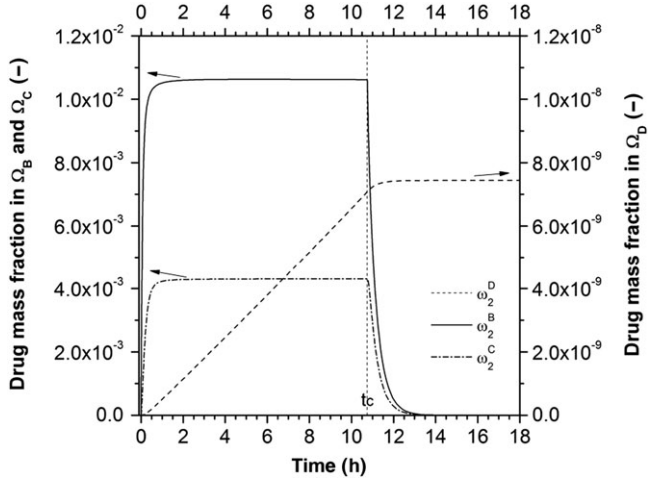

Figure 6

The changes in drug mass fraction in the various domains during the dissolution process for an initial polymer coating thickness of 20 µm.

modified model was applied to the systems with pellets of different coating thickness (Figure 7).

The drug release calculated shows a zero-order behaviour for all the types of pellets and during all the dissolution process. Despite the prediction being good in the first hours, the model is not able to properly describe the experimental results when the drug release rate decreases.

Heterogeneous system

Relevance of the PSD of Cellets. The model utilized in this section is constituted by eqs 1–12, 16 and 19–25. Each class of pellets presents its fractional drug release

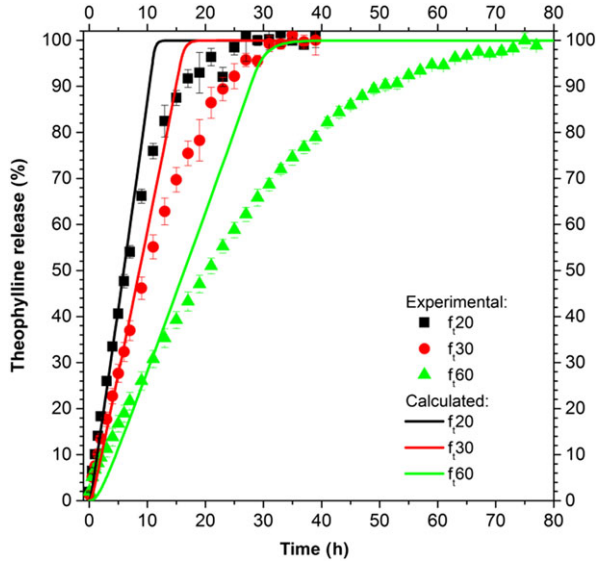

Figure 7

Drug release from ensembles of homogeneous pellets.

that contributes to the average release (i.e. the characteristic release of the dose or, in other terms, the release that would be experimentally recorded). In Figure 8, the results in terms of release from the single class (individuated by eq. 19) as well as in terms of average release from the different polymeric layers are shown. The model parameters were kept the same as in the homogeneous system model.

The drug release from the different classes is minimal, generating an average drug release similar to that of the homogeneous system.

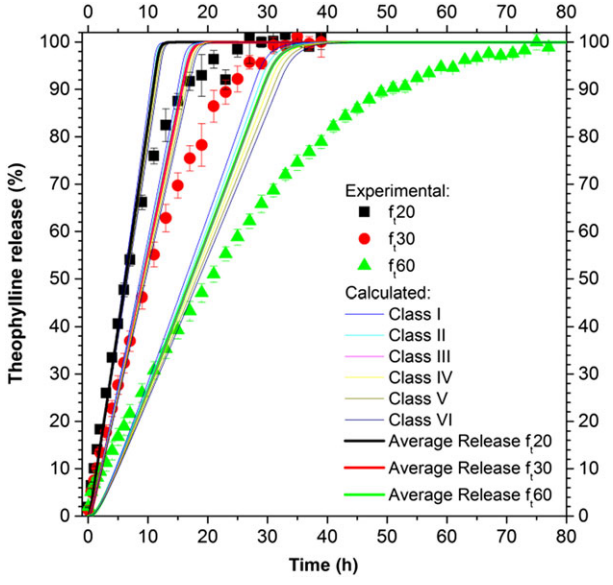

Figure 8

Drug release from ensembles of pellets, where the inert core has a PSD described for the six classes defined by eq. 20.

Relevance of the SD of the coating thickness. The model, based on eqs 1–12, 16 and 23–32, was modified based on the experimental drug release of the pellets with theoretical film thickness of 30 μm (f_t30) (R^2 = 0.995). The transport parameters used were based on those found in the literature or experimentally (Table 1), using as fitting parameters the mean and the standard deviation of the film thickness distribution, μ and σ. The best fitting parameters were $\mu_{fitting} = 20$ μm and $\sigma_{fitting} = 7.5$ μm. The SD of the film thickness is presented in Table 3. The most populated classes, in terms of numerical fraction $n_i/n_{tot}|_{f_t^{mean}(i)}$ (%), are between the second and the sixth classes. The drug release from the ith class, as well as the average release, are shown in Figure 9.

This modelling approach does not require adjustable transport parameters, which were obtained from literature or experiments (Table 1), and requires two parameters for the description of the SD of the film thickness. These last two were successfully related to the initial theoretical film thickness, by considering the results obtained for f_t30, as follows:

$$\mu_{fitting} = \frac{2}{3} f_t$$
$$\sigma_{fitting} = \frac{3}{8} \mu_{fitting} = \frac{1}{4} f_t \quad (33)$$

In this way, a fully predictive model was obtained and tested on the other two systems: f_t20 and f_t60, whose film thickness distribution is reported in Table 3. The modelling results, in terms of average release, are presented in Figure 10 and compared with the experimental data. The agreement is very good for f_t20 (R^2 = 0.991) and satisfactorily good for f_t60 (R^2 = 0.981), confirming that the distribution of the film thickness is a crucial component in the understanding and modelling of drug release from pellets.

Discussion and conclusions

In this work, a mathematical model for predicting drug release from an ensemble of coated pellets was proposed, implemented and successfully compared with experimental results. A layered lumped parameters modelling approach was used to describe the single-coated pellet behaviour in terms of size and species mass fraction time evolutions. The pellet was assumed to consist of several time-dependent domains representing the inert core, the solid and liquid drug layers and the polymeric film coating. The time evolution of the dimensions of the pellet (Figure 5) shows that the accumulation of water, driven by the concentration difference between the external medium and the internal liquid layer, generates a volumetric deformation of the system. In particular, water accumulates inside the pellet promoting the further dissolution of solid drug. This water uptake leads to an overall increase in the size of the pellet and to the stretching of the polymeric film layer, due to its limited swelling ability with respect to the inner part of the pellet. The analysis of the evolution of the drug mass fraction (Figure 6) within the pellet and in the external dissolution medium shows that the presence of water

Table 3

Film thickness distribution

Class	f_t20 $\mu_{fitting} = 13.\bar{3}$ µm $\sigma_{fitting} = 5$ µm $f_t^{mean}(i)$ (µm)	f_t30 $\mu_{fitting} = 20$ µm $\sigma_{fitting} = 7.5$ µm $f_t^{mean}(i)$ (µm)	f_t60 $\mu_{fitting} = 40$ µm $\sigma_{fitting} = 15$ µm $f_t^{mean}(i)$ (µm)	$n_i/n_{tot}\vert_{f_t^{mean}(i)}$ (%)
I	1.95	3.00	6.00	2.71
II	5.85	9.00	18.00	11.20
III	9.75	15.00	30.00	25.18
IV	13.65	21.00	42.00	30.82
V	17.55	27.00	54.00	20.57
VI	21.45	33.00	66.00	7.48
VII	25.35	39.00	78.00	1.48
VIII	29.25	45.00	90.00	0.16
IX	33.15	51.00	102.00	0.01
X	37.05	57.00	114.00	0

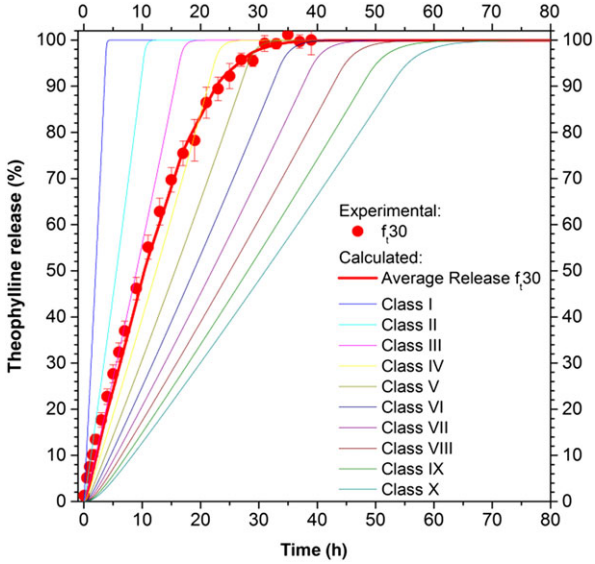

Figure 9

Drug release from an ensemble of pellets with different film thickness distributions.

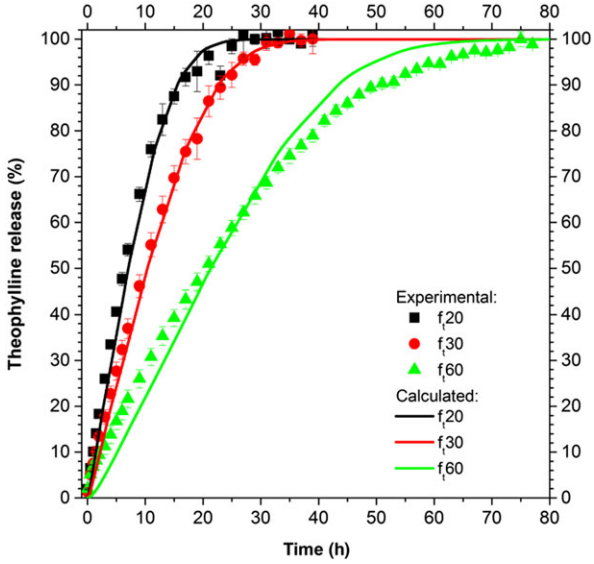

Figure 10

Drug release from ensembles of pellets with various SD of the film thickness and predictive modelling results for f_t20 and f_t60.

within the pellet helps to dissolve the solid drug up to its dissolution limit, a value that is kept constant until the complete dissolution of the solid drug reservoir. This clearly shows that, in this case, the drug dissolution is not a limiting step.

The single pellet model was successively extended to describe ensembles of pellets where different approaches to describe the system polydispersity were hypothesized and implemented. In particular, as the simplest approach, a perfectly homogeneous system of pellets was modelled, from which a drug release kinetic of zero order was obtained, far from the experimental results (Figure 7). To reproduce the experimental sigmoidal drug release results from ensembles of pellets, drug diffusion coefficients as a function of the dissolution time could be used (i.e. Marucci *et al.*, 2013), based on the assumption that morphological changes in the polymeric film modify the diffusion process. However, from our results, which are supported by the morphological analyses pre- and post-dissolution (results not shown) that show the absence of substantial modifications, this approach was rejected and the hypothesis of a perfectly homogeneous system was found to be too simplistic to be able to reproduce the experimental results.

A more realistic modelling approach is to consider the heterogeneity of the ensemble of pellets. This can arise from several factors: the particle SD of the inert core, drug or polymer layer thickness distribution and so forth. In particular, the impact of the PSD of Cellets and the relevance of the polymeric coating thickness distribution were evaluated. The effect of the drug layer thickness distribution was disregarded *a priori*, as the value calculated from the effective mass of drug loaded onto the pellets provided a good estimation of the drug layer thickness. This assumption is justified as we found that this layer is only few micrometres and its distribution around this mean value would not substantially affect the results. In modelling the inert core SD (Figure 8), six classes were used with a different inert core radius, reported in eq. 19. In modelling the film thickness SD (Figure 9 and Table 3), 10 classes were used, which differ in their film thickness dimensions (reported in Table 3).

From analysing the impact of the SD of Cellets (Figure 8), it is evident that the difference in drug release from the different classes is minimal (the pellets in these classes differ only in the size of their Cellets), and the average release does not differ from the drug release obtained when considering a homogenous system. This can be explained by assuming that the mass flow rate of the ith class ($\dot{W}_{2i}$) is proportional to the inert core radius to the power of two, eq. 34. The drug release from the ith class $R_i(t)$, from eq. 36, can be expressed as the product of the drug mass flow rate times the dissolution time t, divided by the initial drug mass in the ith class m_{20i}, eq. 38. This latter value is proportional to the inert core radius to the power of two, eq. 37, similar to the mass flow rate, therefore giving a drug release independent of the inert core radius, eq. 38.

$$\begin{aligned}\dot{W}_{2_i} &\sim k\Delta\omega_2 4\pi R_{C,i}^2 \\ &= k\Delta\omega_2 4\pi(R_{0i}+\delta_A+\delta_B+\delta_C)^2 \approx k\Delta\omega_2 4\pi\left[R_{0_i}^2+2R_{0i}(\delta_A+\delta_B+\delta_C)\right] = \\ &= k\Delta\omega_2 4\pi\left[R_{0_i}^2+2R_{0i}(R_{Ci}-R_{0i})\right] \\ &= k\Delta\omega_2 4\pi R_{0_i}^2\left[2\frac{R_{Ci}}{R_{0i}}-1\right] \approx k\Delta\omega_2 4\pi R_{0_i}^2\end{aligned} \tag{34}$$

$$m_{2i}(t) = m_{20i} - \dot{W}_{2i}t \tag{35}$$

$$R_i(t) = \frac{m_{20i} - m_{2i}}{m_{20i}} = \frac{\dot{W}_{2i}}{m_{20i}}t \tag{36}$$

$$\begin{aligned}m_{20i} &= \omega_{20}\rho_A\frac{4}{3}\pi\left(R_{A0_i}^3 - R_{0_i}^3\right) \\ &= \omega_{20}\rho_A\frac{4}{3}\pi\left[(R_{0i}+\delta_{A0})^3 - R_{0_i}^3\right] \approx \omega_{20}\rho_A\frac{4}{3}\pi R_{0_i}^2\delta_{A0}\end{aligned} \tag{37}$$

$$R_i(t) \approx \frac{k\Delta\omega_2 4\pi}{\omega_{20}\rho_A\frac{4}{3}\pi\delta_{A0}}t \tag{38}$$

From this analysis, it is evident that the PSD of Cellets, under the hypotheses of homogeneous drug and polymer layers thickness within the classes, has a negligible impact on the pellets produced. However, inert cores with narrow PSD should always be preferred since they are easier to fluidize and can ensure a more homogeneous layering.

From the analysis of the impact of the SD of the polymeric film thickness on the drug release (Figure 9), it can be seen that the classes of pellets with a lower film thickness promptly release the theophylline, while the release rate decreases with an increase in film thickness. The resulting average release, which was obtained from the results of all the classes, is able to reproduce the experimental results that deviate from a zero-order release behaviour. Similarly, Donbrow *et al*. (1988) using a simple statistical model (in which the distribution of up to three parameters was assumed and arbitrarily varied: payload, payload release time and release rate constant), theoretically demonstrated that the ensemble release rate, different from a kinetic of zero order, could be obtained from single pellets release of zero order, by considering the parameters of the distribution of the ensemble. In the present study, by using a mechanistic model and analysing the distribution of physical properties (inert core dimension and film thickness distribution), it has been demonstrated that some features (i.e the film thickness distribution) could have more impact than others (i.e. inert core radius) on the drug release behaviour.

The drug release from an ensemble of pellets with a theoretical film thickness of 30 μm (f_t30) was initially described (Figure 9) by using only the film thickness dimension (average thickness and its standard deviation, assuming a Gaussian distribution) as a fitting parameter. The values of the fitting parameters resulting from the optimization procedure were successfully related to the theoretical film thickness, eq. 33, and demonstrated that the average thickness able to describe the drug release was lower than the theoretical thickness, as for the drug coating, confirming that the experimental efficiency of layering was lower than one. Moreover, the correlation with the theoretical thickness allowed us to obtain a predictive model capable of describing the drug release from other ensembles of pellets with a different theoretical film thickness (Figure 10), demonstrating that the right physical phenomena were considered and described.

In conclusion, in this work, a mechanistic model for the description of drug release from a single coated pellet as well as from a polydispersed ensemble of pellets was developed, implemented and successfully compared with experimental results. Both the models, the single pellet model and the ensemble of pellets model, could be successfully used to describe and predict the drug release from these systems. Moreover, the results of the ensemble of pellets model clearly demonstrated that the SD of the inert core has a minimal impact on the drug release, whereas the polymeric film thickness distribution plays the major role, indicating that it is a key parameter to control in the production of pellets-based drug delivery systems.

Author contributions

D.C. contributed to establish the model, wrote the code and runs the simulations; M.M.C. performed the experiments and analysed the data; A.A.B. supervised the modelling work

and organized the data; J.K. organized the experimental work; A.L. had the basic idea, organized the experiments and supervised the experimental work; G.L. contributed to establish the model and organized optimization strategies. All the authors contributed in the writing and in the editing of the manuscript.

Conflict of interest

The authors declare no conflicts of interest.

Declaration of transparency and scientific rigour

This Declaration acknowledges that this paper adheres to the principles for transparent reporting and scientific rigour of preclinical research recommended by funding agencies, publishers and other organisations engaged with supporting research.

References

Abrahamsson B, Alpsten M, Jonsson UE, Lundberg PJ, Sandberg A, Sundgren M *et al.* (1996). Gastro-intestinal transit of a multiple-unit formulation (metoprolol CR/ZOK) and a non-disintegrating tablet with the emphasis on colon. Int J Pharm 140: 229–235.

Bird RB, Stewart WE, Lightfoot EN (2007). Transport Phenomena. Wiley: USA.

Borgquist P, Nevsten P, Nilsson B, Wallenberg LR, Axelsson A (2004). Simulation of the release from a multiparticulate system validated by single pellet and dose release experiments. J Control Release 97: 453–465.

Borgquist P, Zackrisson G, Nilsson B, Axelsson A (2002). Simulation and parametric study of a film-coated controlled-release pharmaceutical. J Control Release 80: 229–245.

Caccavo D, Cascone S, Lamberti G, Barba AA (2015). Controlled drug release from hydrogel-based matrices: experiments and modeling. Int J Pharm 486: 144–152.

Dappert T, Thies C (1978). Statistical models for controlled release microcapsules: rationale and theory. J Membr Sci 4: 99–113.

Donbrow M, Hoffman A, Benita S (1988). Variation of population release kinetics in polydisperse multiparticulate systems (microcapsules, microspheres, droplets, cells) with heterogeneity of one, two or three parameters in the population of individuals. J Pharm Pharmacol 40: 93–96.

Grassi M, Colombo I, Lapasin R (2000). Drug release from an ensemble of swellable crosslinked polymer particles. J Control Release 68: 97–113.

Grassi M, Colombo I, Lapasin R (2001). Experimental determination of the theophylline diffusion coefficient in swollen sodium-alginate membranes. J Control Release 76: 93–105.

Grassi M, Grassi G, Lapasin R, Colombo I (2006). Understanding drug release and absorption mechanisms: a physical and mathematical approach. CRC Press: Boca Raton, FL, USA.

Gross ST, Hoffman A, Donbrow M, Benita S (1986). Fundamentals of release mechanism interpretation in multiparticulate systems – the prediction of the commonly observed release equations from statistical population-models for particle ensembles. Int J Pharm 29: 213–222.

Holz M, Heil SR, Sacco A (2000). Temperature-dependent self-diffusion coefficients of water and six selected molecular liquids for calibration in accurate 1H NMR PFG measurements. Phys Chem Chem Phys 2: 4740–4742.

Kaunisto E, Marucci M, Borgquist P, Axelsson A (2011). Mechanistic modelling of drug release from polymer-coated and swelling and dissolving polymer matrix systems. Int J Pharm 418: 54–77.

Manca D, Rovaglio M (2003). Modeling the controlled release of microencapsulated drugs: theory and experimental validation. Chem Eng Sci 58: 1337–1351.

Marucci M, Andersson H, Hjartstam J, Stevenson G, Baderstedt J, Stading M *et al.* (2013). New insights on how to adjust the release profile from coated pellets by varying the molecular weight of ethyl cellulose in the coating film. Int J Pharm 458: 218–223.

Noyes AA, Whitney WR (1897). The rate of solution of solid substances in their own solutions. J Am Chem Soc 19: 930–934.

Serajuddin ATM, Jarowski CI (1985). Effect of diffusion layer pH and solubility on the dissolution rate of pharmaceutical acids and their sodium salts II: salicylic acid, theophylline, and benzoic acid. J Pharm Sci 74: 148–154.

Shampine LF, Reichelt MW (1997). The MATLAB ODE suite. Siam J Sci Comput 18: 1–22.

Siepmann F, Siepmann J, Walther M, MacRae RJ, Bodmeier R (2008). Polymer blends for controlled release coatings. J Control Release 125: 1–15.

Supporting Information

Additional Supporting Information may be found online in the supporting information tab for this article.

http://doi.org/10.1111/bph.13776

Data S1 MATLAB code in PDF format.
Data S2 Whole dose of pellets (film thickness SD) - MATLAB code in TXT format.
Data S3 Whole dose of pellets (cellets SD) - MATLAB code in TXT format.
Data S4 Single pellet model - MATLAB code in TXT format.